



Published in final edited form as:

J Alzheimers Dis Parkinsonism. 2016 June ; 6(3): . doi:10.4172/2161-0460.1000238.

Targeting Alzheimer's Disease Neuro-Metabolic Dysfunction with a Small Molecule Nuclear Receptor Agonist (T3D-959) Reverses Disease Pathologies

Ming Tong^{1,2,4}, Cesar Dominguez⁸, John Didsbury⁹, and Suzanne M de la Monte^{1,2,3,4,5,6,7,*}

¹Liver Research Center, Warren Alpert Medical School of Brown University, Providence, RI, USA

²Divisions of Gastroenterology, Warren Alpert Medical School of Brown University, Providence, RI, USA

³Department of Neuropathology, Warren Alpert Medical School of Brown University, Providence, RI, USA

⁴Department of Medicine, Warren Alpert Medical School of Brown University, Providence, RI, USA

⁵Department of Pathology, Warren Alpert Medical School of Brown University, Providence, RI, USA

⁶Department of Neurology, Warren Alpert Medical School of Brown University, Providence, RI, USA

⁷Department of Neurosurgery, Rhode Island Hospital and the Warren Alpert Medical School of Brown University, Providence, RI

⁸Williams College, Williams, MA, USA

⁹T3D Pharmaceuticals, Raleigh Durham, NC, USA⁵Australian School of Advanced Medicine, Macquarie University, Sydney, Australia

Abstract

Background—Alzheimer's disease (AD) could be regarded as a brain form of diabetes since insulin resistance and deficiency develop early and progress with severity of neurodegeneration. Preserving insulin's actions in the brain restores function and reduces neurodegeneration.

T3D-959 is a dual nuclear receptor agonist currently in a Phase 2a trial in mild-to-moderate AD patients (ClinicalTrials.gov identifier NCT02560753). Herein, we show that T3D-959 improves motor function and reverses neurodegeneration in a sporadic model of AD.

Methods—Long Evans rats were administered intracerebral (i.c.) streptozotocin (STZ) or normal saline (control) and dosed orally with T3D-959 (1.0 mg/kg/day) or saline for 21 or 28 days.

This is an open-access article distributed under the terms of the Creative Commons Attribution License, which permits unrestricted use, distribution, and reproduction in any medium, provided the original author and source are credited.

*Corresponding author: Suzanne M de la Monte, Pierre Galletti Research Building, Rhode Island Hospital, 55 Claverick Street, Room 419, Providence, RI, USA, Tel: 401-444-7364; Fax: 401-444-2939; Suzanne_DeLaMonte_MD@Brown.edu.

Rotarod tests evaluated motor function. Histopathology with image analysis was used to assess neurodegeneration.

Results—T3D-959 significantly improved motor performance, and preserved both cortical and normalized white matter structure in i.c STZ-treated rats. T3D-959 treatments were effective when dosed therapeutically, whether initiated 1 day or 7 days after i.c. STZ.

Conclusion—T3D-959's targeting neuro-metabolic dysfunctions via agonism of PPAR delta and PPAR gamma nuclear receptors provides potential disease modification in AD.

Keywords

Alzheimer; T3D-959; PPAR agonist; Type 3 diabetes; Streptozotocin; Motor function; Cerebellum; Neurodegeneration

Introduction

Effective disease modifying therapy is critically needed for the treatment of Alzheimer's disease (AD). Despite extensive research and large-scale, long-term treatment with drugs that target symptoms including acetylcholinesterase inhibitors, NMDA receptor antagonists and amyloid vaccines, the clinical course of AD has not been significantly remediated. The most likely explanation for these failures is that AD multifaceted and is caused by inter-related cellular, biochemical and molecular abnormalities that culminate in loss of neurons, deposition of amyloid beta, accumulation of phospho-tau-containing neuronal cytoskeletal lesions, activation of cell death cascades, deficits in energy metabolism, mitochondrial dysfunction, increased inflammation, DNA damage and oxidative stress. Importantly, these pathophysiological responses closely resemble effects of insulin resistance and insulin deficiency as occur in diabetes mellitus, except the alterations selectively or predominantly affect the brain. This concept regarding the pathogenesis of AD as a consequence of neuro-metabolic dysfunction led to the term 'Type-3 Diabetes' [1,2]. Correspondingly, the earliest abnormalities, preceding the onset of cognitive impairment, include impairments in glucose utilization and energy metabolism [3–5].

After the brain is totally dependent on glucose as an energy source, and reduced brain glucose metabolism is both a hallmark of AD and the future best predictor of cognitive decline [6–9]. Insulin is needed for efficient utilization of glucose by brain cells, and is the master hormone whose signaling regulates major biological responses including: Cell growth, neuronal and oligodendroglial survival, neuronal plasticity, energy metabolism, acetylcholine production, inhibition of oxidative stress, and myelin maintenance. Reductions in brain insulin signaling due to insulin deficiency or insulin receptor resistance could account for the majority of molecular, biochemical, and histopathological lesions, as well as cognitive impairment in AD [2,10–18]. Furthermore, disruption of neuronal insulin signaling networks enhances apoptosis [19,20], promotes oxidative injury induced by A β _{1–42} [21], increases secretion of A β _{1–42} [22], blocks removal of extracellular A β -oligomers [23] and increases plaque burden [24].

Growing evidence suggests that brain insulin resistance promotes or triggers key pathologies in AD [2,3,11,25–34], corresponding with the observed changes in levels of insulin

signaling molecules in AD forebrains and associated declines in memory [2,11,12,27,32,34–36]. What is particularly alarming is that peripheral insulin resistance, as occurs in Type 2 diabetes mellitus (T2DM), contributes to AD and cognitive impairment by reducing brain insulin uptake and increasing brain levels of A β , tau-phosphorylation, oxidative stress, pro-inflammatory cytokines, advanced glycation end products, dyslipidemia, and apoptosis [12,13,37–41]. However, AD shares many pathophysiological features including insulin resistance, oxidative stress, inflammation amyloid aggregation and cognitive impairment with T2DM and other peripheral insulin resistance diseases such as metabolic syndrome and non-alcoholic fatty liver disease [25,26,37,42,43], yet these disease processes can occur independently or overlap with one another. One consideration is that insulin resistance diseases share the same or similar underlying causes, but individual factors govern the targeting of specific organ-systems.

Given the spectrum of abnormalities in AD, disease remediation will likely require treatment of multiple molecular and biochemical targets [44]. Peroxisome proliferator-activated receptors (PPARs) are nuclear hormone receptors that function as transcription factors and regulate gene expression [45–48]. PPAR- β/δ , the primary target of T3D-959, are highly expressed in brain, and PPAR- γ , the secondary target of T3D-959, is widely expressed throughout the body. Hetero-dimerization of PPARs with retinoid x receptors regulates target genes [45–48], and the attendant alterations in intracellular signaling enhance energy metabolism, cell growth and differentiation, and inhibit inflammation and oxidative stress [49–53]. Since previous studies showed that PPAR- β/δ agonists can effectively treat experimental STZ [10,54] and 5XFAD [55] models of AD, such agonists are attractive therapeutic targets for AD. Since PPAR- β/δ is abundantly expressed in the brain, and both PPAR- β/δ and PPAR- γ [56,57] agonists exhibit therapeutic efficacy in experimental AD models, dual activation of their receptors may provide enhanced therapeutic benefit in humans with AD.

T3D-959 is a brain penetrating dual nuclear receptor agonist in which PPAR- δ is the primary target (human ED₅₀=19 nM) while PPAR- γ is the secondary target (human ED₅₀=297 nM). In a previous study, we demonstrated efficacy of T3D-959 for preserving spatial learning and memory and preventing cellular and molecular indices of neurodegeneration in an established experimental model of sporadic AD [54]. The present work characterizes the structural and functional therapeutic effects of T3D-959 on i.c. STZ-induced cerebellar degeneration in the same model.

The cerebellum was studied because it is targeted by neurodegeneration in AD [2,58], insulin signaling is an important regulator of cerebellar structure and function [59], and the cerebellum is a major target of brain insulin resistance, irrespective of cause [17,18,30,44,59–62]. Since 1999, at least 53 human research articles have been published demonstrating that besides its role in coordination of voluntary movement, gait, posture, speech and motor function, the cerebellum helps control cognitive functions that require precise timing and behavior [63–67]. It is also believed that cell loss in the cerebellum could be related to coordination deficits that often occur in mid-to-late stages of AD [67–71]. The present work was designed to increase understanding of the nature and degree to which a

novel δ/γ PPAR agonist might be beneficial for treating or reducing severity of neurodegeneration in structural targets of brain insulin resistance in AD.

Methods

Intracerebral Streptozotocin (STZ)

Intracerebral (i.c.) treatment with STZ was used to cause brain metabolic dysfunction and insulin resistance as occur in human sporadic AD [3,16]. Long Evans male and female rats (8–12/group) were anesthetized by intraperitoneal (i.p.) injection of ketamine (100 mg/kg)/xylazine (10 mg/kg) and administered i.c. STZ (0.9 mg/kg) or saline (1–2 μ L volumes) into the lateral ventricle (1 mm caudal, 2 mm lateral to the bregma) as previously described [72]. Rats were administered 5 mL/kg of subcutaneous sterile saline to avoid post-operative dehydration, and kept warm using a temperature-controlled blanket until they were fully recovered.

Formulation and administration

T3D-959 was formulated as a solution in 0.9% NaCl at a concentration of 4.44 mg/ml and prepared fresh daily. Rats were treated by oral gavage with 1.0 mg/kg T3D-959 or normal saline vehicle, once daily from 1 day or 7 days after the i.c. STZ or vehicle treatments. Oral gavage was performed using a ball ended feeding needle to inject drug or vehicle.

Rotarod studies

We used rotarod tests to assess long-term effects of i.c. STZ treatment and the therapeutic effects of T3D-959 on motor function [73]. Rats were administered 10 trials at incremental speeds up to 10 rpm, with 10 min rest between trials. The latency to fall was automatically detected and recorded with photocells placed over the rod. Trials were stopped after 30 s to avoid exercise fatigue. Data from trials 1–3 (2–5 rpm), 4–7 (5–7 rpm), and 8–10 (8–10 rpm) were culled and analyzed using the Mann-Whitney test.

Histological and image analysis studies

The rats were sacrificed by isoflurane inhalation. Cerebella were cut in the mid-sagittal plane, weighed, immersion fixed in 10% formalin, and embedded in paraffin. Histological sections (4 μ m thick) generated 5 mm from the midline were stained with Luxol Fast Blue, hematoxylin and eosin (LHE) and used for histopathological assessments and image analysis. Assessments of regional brain atrophy can be achieved by several approaches that may differ in sensitivity, including measurement of cortical thickness and cross-sectional area [74]. Therefore, two approaches were used to extract information about cortical and white matter thicknesses in relation to i.c. STZ and T3D-959 treatment: 1) image analysis to measure cross-sectional areas; and 2) semi-quantitative assessments of cortical and white matter thicknesses and cellularity within the granule and Purkinje cell layers. ImageJ/Fiji was used to determine cross-sectional areas of the entire slice, molecular and granule cell layers, and white matter (Figure 1). In addition, histological sections were scored with respect to uniformity of thickness or cellularity of the molecular, granule cell, Purkinje cell, and white matter regions of the vermis using a semi-quantitative grading system (Table 1). All slides analyses were performed under code.

Statistics

Graphs depict group means and standard deviations. Inter-group comparisons were made using one-way or two-way analysis of variance (ANOVA) and the Tukey post hoc test (GraphPad Prism 6, San Diego, CA).

Results

T3D-959 treatments restore i.c. STZ-mediated impairments of motor function

Rotarod data were grouped and analyzed using the Mann-Whitney test. With increasing difficulty of the trials (based on rotation speed of the rod), latency to fall declined in all groups (Figure 2). However, with regard to the least challenging series of trials (#1–#4), the mean latency to fall was significantly reduced by i.c. STZ relative to control (Figure 2A). Treatment with T3D-959 improved performance in the STZ group, but the difference relative to control was still significant. For intermediate-level trials (#5–#7), T3D-959 treatment significantly increased mean latency to fall in both control and STZ-exposed rats relative to corresponding vehicle-treated rats (Figure 2B). For the most challenging group of trials (#8–#10), latency to fall was significantly shorter in the STZ-exposed relative to the other 3 groups, and performances of vehicle-treated controls, T3D-959 treated controls, and T3D-959 treated STZ-exposed rats were similar to each other (Figure 2C).

T3D-959 effects on STZ-associated cerebellar degeneration

There were no statistically significant inter-group differences in the mean cerebellar weights (Figure 3A), or the mean relative cross-sectional areas of the molecular (Figure 3B) or granule (Figure 3C) cell layers. In contrast, i.c. STZ significantly reduced the mean relative cross-sectional area of white matter. Treatment with T3D-959 from 1 or 7 days after i.c. STZ prevented white matter atrophy; however, the 7 day delayed treatment results more closely approximated the findings in controls (Figure 3D).

T3D-959 effects on STZ-mediated cerebellar histopathology

Although the image analysis of cross-sectional areas demonstrated white matter atrophy in the i.c. STZ group and therapeutic responses to T3D-959, visual inspection of the histopathology revealed clear inter-group differences in cortical layer cellularity and thickness that were not detected by that approach. Therefore, systematic analysis (Figure 4) and scoring (Figure 5) of cellular pathology in the cerebellar vermis under code was used to provide more detailed assessments of i.c. STZ's effects and the therapeutic responses to T3D-959. In all samples, the cerebellar architecture had the expected organization including an outer molecular layer, middle Purkinje cell layer, and thick, densely populated granule cell layer with clearly delineated white matter cores. In controls, the cerebellar architecture was relatively uniform within each layer and exhibited minimal or no evidence of cell injury or loss (Figures 4A and 4E). The i.c.-STZ treatment caused cortical atrophy with thinning of the molecular layer, reduced populations of Purkinje cells with large gaps corresponding to regions of neuronal loss, as well as multiple neurons exhibiting shrinkage and eosinophilia reflecting ongoing necrosis. In addition, i.c. STZ caused irregular thinning of the granule cell layer and white matter cores (Figures 4B and 4F). T3D-959 treatments initiated either 1

day or 7 days post i.c. STZ increased the molecular layer thickness, reduced neuronal loss and necrosis in the Purkinje layer, and expanded the white matter core thickness (Figures 4C, 4D, 4G and 4H). But, did not restore the thickness of the granule cell layer. Although T3D treatment conspicuously increased cell density within the granule layer, the granule cell layer thickness remained irregularly thinned. These results suggest that T3D may be neuroprotective for both granule and Purkinje cells.

Semi-quantitative histological grading of cerebellar structure

Since the histological abnormalities in the cortex were not well reflected by the image analysis results, we evaluated the tissue sections using a semi-quantitative grading scheme to systematically assess effects of STZ and T3D treatments on cerebellar vermis architecture (Table 1). H&E stained sections of cerebellar vermis were scored under code using semi-quantitative assessments (Table 1). The mean \pm S.D. scores corresponding to uniformity and thickness of the molecular layer, cellularity of the Purkinje layer, and thickness and cellularity of the granule cell layer are depicted in Figure 5. Two-way ANOVA demonstrated significant inter-group differences with respect to all three regions of cortex. STZ treatment significantly reduced the thickness and uniformity of the molecular layer, and cellularity in the Purkinje and granule cell layers relative to control (Figure 5). The differences in molecular layer thickness and Purkinje cellularity relative to control remained significant for the group that was treated with T3D-959 beginning 1 day after i.c. STZ. However, cellularity and thickness uniformity of the granule cell layer were restored by early treatment with T3D-959. Furthermore, T3D-959 treatment beginning 7 days after i.c. STZ restored or preserved the integrity of all three cortical layers relative to control.

Discussion

Since 2005, over 60 published works have shown that the i.c. STZ model of brain diabetes mimics most aspects of sporadic AD with respect to molecular, biochemical, histopathological, and/or neurobehavioral abnormalities [1,54,75–78]. In this regard, the i.c. STZ model causes amyloid- β deposition, pTau accumulation, cortical-limbic pathway degeneration, deficits in spatial learning and memory, neuro-inflammation, and oxidative stress in the brain, including in regions that are characteristically damaged in AD. In addition, the data show the importance of brain insulin resistance as a mediator of neurodegeneration and amyloid deposition, and vice versa [28,29,36,44,79,80].

AD like diabetes mellitus is associated with insulin resistance, except brain rather than skeletal muscle is the principal organ. In the brain, insulin is a key regulator of glucose utilization and signal transduction networks that mediate cell growth, plasticity, metabolism, neuronal survival, myelin maintenance and acetylcholine biosynthesis, and it inhibits oxidative stress and apoptosis [1,14,15,30,44,59]. Proof of principle for this concept has been provided by experiments in which i.c. administration of STZ, a pro-diabetes toxin, was shown to cause AD-type neurodegeneration [16], and early treatment with PPAR agonists was demonstrated to prevent cognitive impairment and neurodegeneration [10]. The PPAR- δ agonist proved to be considerably more neuroprotective in preserving cognitive function and

hippocampal/temporal lobe structure compared with the PPAR- γ agonist [10], corresponding with the greater abundance of δ versus γ receptor expression in brain [55].

A major advantage of PPAR agonists is that they mediate their effects within the nucleus, circumventing impairments in insulin signaling caused by reductions in surface receptor binding and receptor tyrosine kinase activation, which are features of AD [2,11]. The neuroprotective effects of PPAR- δ and PPAR- γ agonists overlap but are non-identical with respect to downstream insulin-responsive targets [45–48]. T3D-959 is small molecule hybrid PPAR- δ/γ agonist that can be administered as a once daily oral dose and exhibits a high degree of CNS penetrance.

PPAR agonists of all classes that bind to nuclear hormone receptors can cause cellular harm at high concentrations a purported selective. In the manuscript by Peri et al. [81] and another by Rohn et al. [82], the concentrations of PPAR- γ agonist at high caused neuronal apoptosis at 10 micro-M but not 500 nM. Our experimental conditions produced nM tissue concentrations of T3D-959 [54]. Interestingly, the manuscript by Rohn et al. [82] does show nice neurite process extension and improved neuronal viability at the lowest doses of the PPAR γ agonist used, 15-PGJ2. Furthermore, 15d-PGJ2 [82] is not a selective PPAR γ agonist as it also interacts with GPR44; acting through this receptor inhibits hair growth. The high doses of 15d-PGJ2 needed to induce apoptosis are not biologically relevant and can produce off-target effects. In addition, this compound acts as a PGD2 receptor agonist with an EC₅₀ of 10nM, and can have PPAR γ -independent effects [83], calling into question the conclusion that the PPAR γ activation caused neuronal apoptosis. In contrast, T3D-959 has been demonstrated to increase cell survival (see Figure 4a and article by Tong et al. [54]).

The preclinical studies reported herein assessed the neurobehavioral effects of T3D-959 in an established model of sporadic AD in which adult Long Evans rats were treated by i.c. STZ which is known to cause neurodegeneration, impairments in brain insulin and insulin-like growth factor (IGF) signaling, and increased oxidative stress [10,16]. In addition to assessing T3D-959's efficacy, we examined responses to early and late therapeutic intervention. The delayed time point of initiating treatment addresses the fact that many people are first diagnosed at clinically intermediate rather than early stages of disease. At the same time, it was important to assess responses to early intervention because as diagnostic tools improve, early treatment protocols will become feasible.

The rotarod tests demonstrated that i.c. STZ impaired cerebellar motor function and that T3D-959 prevented this effect along with neurodegeneration. It was of further interest that these therapeutic responses to T3D-959 were similar and slightly better when treatment was initiated 7 days as opposed to 1 day post i.c. STZ. Histopathological studies demonstrated that the i.c. STZ mediated neuronal loss in Purkinje and granule cell layers and atrophy of white matter were reversed by T3D-959 treatment. Therefore, the neuroprotective effects of T3D-959 correlate with preservation of motor function.

The therapeutic effects of T3D-959 on cerebellar structure and function correspond with the abundant expression of insulin receptors and prominence of insulin signaling networks in the

cerebellum [59]. Previous studies using various experimental models showed that inhibition of insulin signaling in the cerebellum or cerebellar neurons correlates with neuronal loss and impaired motor function [17,60,62]. In addition, earlier studies showed that treatment with a PPAR- δ agonist effectively restored cerebellar structure and function [10], consistent with findings in the present study. An additional novel finding was the reversal of white matter atrophy in T3D-959 treated i.c. STZ exposed rats. This observation is of particular interest because myelin-producing oligodendrocytes are maintained by insulin/IGF signaling, and white matter atrophy is an early feature of AD [84–86]. Altogether, these data suggest that motor impairments mediated by neuronal loss and white matter atrophy in AD may be ameliorated by T3D-959 therapy.

In conclusion, this study demonstrates that T3D-959 has cleared therapeutic and neuroprotective effects in an established model of sporadic AD. The main effects were associated with improved (normalized) motor function and reversal of cerebellar degeneration. Importantly, therapeutic effects occurred even after a delay in treatment, suggesting that individuals with mild or moderate AD would benefit from this highly effective small molecule drug that has the benefit of oral, once-daily delivery.

Acknowledgments

Supported by AA-011431 and AG-049510 from the National Institutes of Health.

References

1. de la Monte SM, Wands JR. Alzheimer's disease is type 3 diabetes-evidence reviewed. *J Diabetes Sci Technol.* 2008; 2:1101–1113. [PubMed: 19885299]
2. Steen E, Terry BM, Rivera EJ, Cannon JL, Neely TR, et al. Impaired insulin and insulin-like growth factor expression and signaling mechanisms in Alzheimer's disease--is this type 3 diabetes? *J Alzheimers Dis.* 2005; 7:63–80. [PubMed: 15750215]
3. Hoyer S. Is sporadic Alzheimer disease the brain type of non-insulin dependent diabetes mellitus? A challenging hypothesis. *J Neural Transm.* 1998; 105:415–422. [PubMed: 9720971]
4. Iwagoff P, Armbruster R, Enz A, Meier-Ruge W. Glycolytic enzymes from human autoptic brain cortex: Normal aged and demented cases. *Mech Ageing Dev.* 1980; 14:203–209. [PubMed: 6259457]
5. Sims NR, Bowen DM, Smith CC, Flack RH, Davison AN, et al. Glucose metabolism and acetylcholine synthesis in relation to neuronal activity in Alzheimer's disease. *Lancet.* 1980; 1:333–336. [PubMed: 6101790]
6. Brown AM, Sheu RK, Mohs R, Haroutunian V, Blass JP. Correlation of the clinical severity of Alzheimer's disease with an aberration in mitochondrial DNA (mtDNA). *J Mol Neurosci.* 2001; 16:41–48. [PubMed: 11345519]
7. Grady CL, Haxby JV, Schlageter NL, Berg G, Rapoport SI. Stability of metabolic and neuropsychological asymmetries in dementia of the Alzheimer type. *Neurology.* 1986; 36:1390–1392. [PubMed: 3762951]
8. Mosconi L. Brain glucose metabolism in the early and specific diagnosis of Alzheimer's disease. FDG-PET studies in MCI and AD. *Eur J Nucl Med Mol Imaging.* 2005; 32:486–510. [PubMed: 15747152]
9. Mosconi L, McHugh PF. FDG- and amyloid-PET in Alzheimer's disease: Is the whole greater than the sum of the parts? *Q J Nucl Med Mol Imaging.* 2011; 55:250–264. [PubMed: 21532539]
10. de la Monte SM, Tong M, Lester-Coll N, Plater M Jr, Wands JR. Therapeutic rescue of neurodegeneration in experimental type 3 diabetes: Relevance to Alzheimer's disease. *J Alzheimers Dis.* 2006; 10:89–109. [PubMed: 16988486]

11. Rivera EJ, Goldin A, Fulmer N, Tavares R, Wands JR, et al. Insulin and insulin-like growth factor expression and function deteriorate with progression of Alzheimer's disease: Link to brain reductions in acetylcholine. *J Alzheimers Dis.* 2005; 8:247–268. [PubMed: 16340083]
12. Talbot K, Wang HY, Kazi H, Han LY, Bakshi KP, et al. Demonstrated brain insulin resistance in Alzheimer's disease patients is associated with IGF-1 resistance, IRS-1 dysregulation and cognitive decline. *J Clin Invest.* 2012; 122:1316–1338. [PubMed: 22476197]
13. Craft S. Insulin resistance syndrome and Alzheimer's disease: Age- and obesity-related effects on memory, amyloid and inflammation. *Neurobiol Aging.* 2005; 26(Suppl 1):65–69. [PubMed: 16266773]
14. Craft S. Insulin resistance syndrome and Alzheimer disease: Pathophysiologic mechanisms and therapeutic implications. *Alzheimer Dis Assoc Disord.* 2006; 20:298–301. [PubMed: 17132977]
15. Craft S. Insulin resistance and Alzheimer's disease pathogenesis: Potential mechanisms and implications for treatment. *Curr Alzheimer Res.* 2007; 4:147–152. [PubMed: 17430239]
16. Lester-Coll N, Rivera EJ, Soscia SJ, Doiron K, Wands JR, et al. Intracerebral streptozotocin model of type 3 diabetes: Relevance to sporadic Alzheimer's disease. *J Alzheimers Dis.* 2006; 9:13–33. [PubMed: 16627931]
17. Schubert M, Brazil DP, Burks DJ, Kushner JA, Ye J, et al. Insulin receptor substrate-2 deficiency impairs brain growth and promotes tau phosphorylation. *J Neurosci.* 2003; 23:7084–7092. [PubMed: 12904469]
18. Schubert M, Gautam D, Surjo D, Ueki K, Baudler S, et al. Role for neuronal insulin resistance in neurodegenerative diseases. *Proc Natl Acad Sci U S A.* 2004; 101:3100–3105. [PubMed: 14981233]
19. Ryu BR, Ko HW, Jou I, Noh JS, Gwag BJ. Phosphatidylinositol 3-kinase-mediated regulation of neuronal apoptosis and necrosis by insulin and IGF-I. *J Neurobiol.* 1999; 39:536–546. [PubMed: 10380075]
20. Tseng YH, Ueki K, Kriauciunas KM, Kahn CR. Differential roles of insulin receptor substrates in the anti-apoptotic functions of insulin-like growth factor-1 and insulin. *J Biol Chem.* 2002; 277:31601–31611. [PubMed: 12082100]
21. Picone P, Giacomazza D, Vetri V, Carrotta R, Militello V, et al. Insulin-activated Akt rescues Aβ₁₋₄₂ oxidative stress-induced cell death by orchestrating molecular trafficking. *Aging Cell.* 2011; 10:832–843. [PubMed: 21624038]
22. Gupta A, Bisht B, Dey CS. Peripheral insulin-sensitizer drug metformin ameliorates neuronal insulin resistance and Alzheimer's-like changes. *Neuropharmacology.* 2011; 60:910–920. [PubMed: 21277873]
23. Zhao WQ, Lacor PN, Chen H, Lambert MP, Quon MJ, et al. Insulin receptor dysfunction impairs cellular clearance of neurotoxic oligomeric Aβ₁₋₄₂. *J Biol Chem.* 2009; 284:18742–18753. [PubMed: 19406747]
24. Matsuzaki T, Sasaki K, Tanizaki Y, Hata J, Fujimi K, et al. Insulin resistance is associated with the pathology of Alzheimer disease: The Hisayama study. *Neurology.* 2010; 75:764–770. [PubMed: 20739649]
25. Zhao WQ, Townsend M. Insulin resistance and amyloidogenesis as common molecular foundation for type 2 diabetes and Alzheimer's disease. *Biochim Biophys Acta.* 2009; 1792:482–496. [PubMed: 19026743]
26. Correia SC, Santos RX, Perry G, Zhu X, Moreira PI, et al. Insulin-resistant brain state: The culprit in sporadic Alzheimer's disease? *Ageing Res Rev.* 2011; 10:264–273. [PubMed: 21262392]
27. Talbot K. O3-02-02: Expression of pIRS-1 (S312 and S616) is elevated in MCI and AD and correlates with cognitive impairment and neurofibrillary pathology. *Alzheimer and Dement.* 2006; 2:S54.
28. Salkovic-Petrisic M, Hoyer S. Central insulin resistance as a trigger for sporadic Alzheimer-like pathology: an experimental approach. *J Neural Transm Suppl.* 2007:217–233. [PubMed: 17982898]
29. Zhao WQ, De Felice FG, Fernandez S, Chen H, Lambert MP, et al. Amyloid beta oligomers induce impairment of neuronal insulin receptors. *FASEB J.* 2008; 22:246–260. [PubMed: 17720802]

30. de la Monte SM. Insulin resistance and Alzheimer's disease. *BMB Rep.* 2009; 42:475–481. [PubMed: 19712582]
31. Tong M, Neusner A, Longato L, Lawton M, Wands JR, et al. Nitrosamine exposure causes insulin resistance diseases: Relevance to type 2 diabetes mellitus, non-alcoholic steatohepatitis and Alzheimer's disease. *J Alzheimers Dis.* 2009; 17:827–844. [PubMed: 20387270]
32. Moloney AM, Griffin RJ, Timmons S, O'Connor R, Ravid R, et al. Defects in IGF-1 receptor, insulin receptor and IRS-1/2 in Alzheimer's disease indicate possible resistance to IGF-1 and insulin signalling. *Neurobiol Aging.* 2010; 31:224–243. [PubMed: 18479783]
33. Kuljis RO, Salkovic-Petrisic M. Dementia, diabetes, Alzheimer's disease, and insulin resistance in the brain: progress, dilemmas, new opportunities and a hypothesis to tackle intersecting epidemics. *J Alzheimers Dis.* 2011; 25:29–41. [PubMed: 21335659]
34. Liu Y, Liu F, Grundke-Iqbal I, Iqbal K, Gong CX. Deficient brain insulin signalling pathway in Alzheimer's disease and diabetes. *J Pathol.* 2011; 225:54–62. [PubMed: 21598254]
35. Griffin RJ, Moloney A, Kelliher M, Johnston JA, Ravid R, et al. Activation of Akt/PKB, increased phosphorylation of Akt substrates and loss and altered distribution of Akt and PTEN are features of Alzheimer's disease pathology. *J Neurochem.* 2005; 93:105–117. [PubMed: 15773910]
36. Ma QL, Yang F, Rosario ER, Ubeda OJ, Beech W, et al. Beta-amyloid oligomers induce phosphorylation of tau and inactivation of insulin receptor substrate via c-Jun N-terminal kinase signaling: Suppression by omega-3 fatty acids and curcumin. *J Neurosci.* 2009; 29:9078–9089. [PubMed: 19605645]
37. Baker LD, Cross DJ, Minoshima S, Belongia D, Watson GS, et al. Insulin resistance and Alzheimer-like reductions in regional cerebral glucose metabolism for cognitively normal adults with prediabetes or early type 2 diabetes. *Arch Neurol.* 2011; 68:51–57. [PubMed: 20837822]
38. Cole AR, Astell A, Green C, Sutherland C. Molecular connexions between dementia and diabetes. *Neurosci Biobehav Rev.* 2007; 31:1046–1063. [PubMed: 17544131]
39. Neumann KF, Rojo L, Navarrete LP, Fariás G, Reyes P, et al. Insulin resistance and Alzheimer's disease: molecular links and clinical implications. *Curr Alzheimer Res.* 2008; 5:438–447. [PubMed: 18855585]
40. Sims-Robinson C, Kim B, Rosko A, Feldman EL. How does diabetes accelerate Alzheimer disease pathology? *Nat Rev Neurol.* 2010; 6:551–559. [PubMed: 20842183]
41. Cholerton B, Baker LD, Craft S. Insulin resistance and pathological brain ageing. *Diabet Med.* 2011; 28:1463–1475. [PubMed: 21974744]
42. Li L, Hölscher C. Common pathological processes in Alzheimer disease and type 2 diabetes: A review. *Brain Res Rev.* 2007; 56:384–402. [PubMed: 17920690]
43. Tan ZS, Beiser AS, Fox CS, Au R, Himali JJ, et al. Association of metabolic dysregulation with volumetric brain magnetic resonance imaging and cognitive markers of subclinical brain aging in middle-aged adults: The Framingham Offspring Study. *Diabetes Care.* 2011; 34:1766–1770. [PubMed: 21680719]
44. de la Monte SM. Brain insulin resistance and deficiency as therapeutic targets in Alzheimer's disease. *Curr Alzheimer Res.* 2012; 9:35–66. [PubMed: 22329651]
45. Gilde AJ, Van Bilsen M. Peroxisome proliferator-activated receptors (PPARs): Regulators of gene expression in heart and skeletal muscle. *Acta Physiol Scand.* 2003; 178:425–434. [PubMed: 12864748]
46. Kliewer SA, Lehmann JM, Milburn MV, Willson TM. The PPARs and PXR: Nuclear xenobiotic receptors that define novel hormone signaling pathways. *Recent Prog Horm Res.* 1999; 54:345–367. [PubMed: 10548883]
47. Schoonjans K, Staels B, Auwerx J. The peroxisome proliferator activated receptors (PPARs) and their effects on lipid metabolism and adipocyte differentiation. *Biochim Biophys Acta.* 1996; 1302:93–109. [PubMed: 8695669]
48. Lee CH, Olson P, Evans RM. Mini review: Lipid metabolism, metabolic diseases, and peroxisome proliferator-activated receptors. *Endocrinology.* 2003; 144:2201–2207. [PubMed: 12746275]
49. Fuentes L, Roszer T, Ricote M. Inflammatory mediators and insulin resistance in obesity: Role of nuclear receptor signaling in macrophages. *Mediators Inflamm.* 2010; 2010:219583. [PubMed: 20508742]

50. Glass CK, Saijo K. Nuclear receptor transrepression pathways that regulate inflammation in macrophages and T cells. *Nat Rev Immunol.* 2010; 10:365–376. [PubMed: 20414208]
51. de la Monte SM, Tong M, Wands JR. Therapeutic rescue of alcoholic neurodegeneration with PPAR agonists. 2010
52. Deplanque D, Gele P, Petrault O, Six I, Furman C, et al. Peroxisome proliferator-activated receptor- α activation as a mechanism of preventive neuroprotection induced by chronic fenofibrate treatment. *J Neurosci.* 2003; 23:6264–6271. [PubMed: 12867511]
53. Sivarajah A, Chatterjee PK, Patel NS, Todorovic Z, Hattori Y, et al. Agonists of peroxisome-proliferator activated receptor- γ reduces renal ischemia/reperfusion injury. *Am J Nephrol.* 2003; 23:267–276. [PubMed: 12840602]
54. Tong M, Deochand C. T3D-959: A multi-faceted disease remedial drug candidate for the treatment of Alzheimer's disease. *J Alzheimers Dis.* 2016; 51:123–138. [PubMed: 26836193]
55. Kalinin S, Richardson JC, Feinstein DL. A PPAR δ agonist reduces amyloid burden and brain inflammation in a transgenic mouse model of Alzheimer's disease. *Curr Alzheimer Res.* 2009; 6:431–437. [PubMed: 19874267]
56. Rodriguez-Rivera J, Denner L, Dineley KT. Rosiglitazone reversal of Tg2576 cognitive deficits is independent of peripheral gluco-regulatory status. *Behav Brain Res.* 2011; 216:255–261. [PubMed: 20709114]
57. Searcy JL, Phelps JT, Pancani T, Kadish I, Popovic J, et al. Long-term pioglitazone treatment improves learning and attenuates pathological markers in a mouse model of Alzheimer's disease. *J Alzheimers Dis.* 2012; 30:943–961. [PubMed: 22495349]
58. Wegiel J, Wisniewski HM, Dziewiatkowski J, Badmajew E, Tarnawski M, et al. Cerebellar atrophy in Alzheimer's disease-clinicopathological correlations. *Brain Res.* 1999; 818:41–50. [PubMed: 9914436]
59. de la Monte SM, Wands JR. Review of insulin and insulin-like growth factor expression, signaling, and malfunction in the central nervous system: relevance to Alzheimer's disease. *J Alzheimers Dis.* 2005; 7:45–61. [PubMed: 15750214]
60. de la Monte SM, Tong M, Bowling N, Moskal P. si-RNA inhibition of brain insulin or insulin-like growth factor receptors causes developmental cerebellar abnormalities: relevance to fetal alcohol spectrum disorder. *Mol Brain.* 2011; 4:13. [PubMed: 21443795]
61. Grünblatt E, Hoyer S, Riederer P. Gene expression profile in streptozotocin rat model for sporadic Alzheimer's disease. *J Neural Transm (Vienna).* 2004; 111:367–386. [PubMed: 14991460]
62. Xu J, Yeon JE, Chang H, Tison G, Chen GJ, et al. Ethanol impairs insulin-stimulated neuronal survival in the developing brain: Role of PTEN phosphatase. *J Biol Chem.* 2003; 278:26929–26937. [PubMed: 12700235]
63. Chételat G, Villemagne VL, Villain N, Jones G, Ellis KA, et al. Accelerated cortical atrophy in cognitively normal elderly with high β -amyloid deposition. *Neurology.* 2012; 78:477–484. [PubMed: 22302548]
64. Dos Santos V, Thomann PA, Wüstenberg T, Seidl U, Essig M, et al. Morphological cerebral correlates of CERAD test performance in mild cognitive impairment and Alzheimer's disease. *J Alzheimers Dis.* 2011; 23:411–420. [PubMed: 21116054]
65. Farrow TF, Thiyagesh SN, Wilkinson ID, Parks RW, Ingram L, et al. Fronto-temporal-lobe atrophy in early-stage Alzheimer's disease identified using an improved detection methodology. *Psychiatry Res.* 2007; 155:11–19. [PubMed: 17399959]
66. Baloyannis SJ. Golgi apparatus and protein trafficking in Alzheimer's disease. *J Alzheimers Dis.* 2014; 42(Suppl 3):S153–162. [PubMed: 24946873]
67. Olazarán J, Hernández-Tamames JA, Molina E, García-Polo P, Dobato JL, et al. Clinical and anatomical correlates of gait dysfunction in Alzheimer's disease. *J Alzheimers Dis.* 2013; 33:495–505. [PubMed: 23011219]
68. Engel PA, Grunnet M. Atypical dementia and spastic paraplegia in a patient with primary lateral sclerosis and numerous necortical beta amyloid plaques: new disorder or Alzheimer's disease variant? *J Geriatr Psychiatry Neurol.* 2000; 13:60–64. [PubMed: 10912726]
69. Gutzmann H, Köhl KP. Emotion control and cerebellar atrophy in senile dementia. *Arch Gerontol Geriatr.* 1987; 6:61–71. [PubMed: 2884937]

70. Ishii K. Clinical application of positron emission tomography for diagnosis of dementia. *Ann Nucl Med.* 2002; 16:515–525. [PubMed: 12593416]
71. Lomoio S, Lopez-Gonzalez I, Aso E, Carmona M, Torrejon-Escribano B, et al. Cerebellar amyloid-beta plaques: Disturbed cortical circuitry in AbetaPP/PS1 transgenic mice as a model of familial Alzheimer's disease. *J Alzheimers Dis.* 2012; 31:285–300. [PubMed: 22561329]
72. Cetin A, Komai S, Eliava M, Seeburg PH, Osten P. Stereotaxic gene delivery in the rodent brain. *Nat Protoc.* 2006; 1:3166–3173. [PubMed: 17406580]
73. Hamm RJ, Pike BR, O'Dell DM, Lyeth BG, Jenkins LW. The rotarod test: an evaluation of its effectiveness in assessing motor deficits following traumatic brain injury. *J Neurotrauma.* 1994; 11:187–196. [PubMed: 7932797]
74. Redolfi A, Manset D, Barkhof F, Wahlund LO, Glatard T, et al. Head-to-head comparison of two popular cortical thickness extraction algorithms: A cross-sectional and longitudinal study. *PLoS One.* 2015; 10:e0117692. [PubMed: 25781983]
75. Paidi RK, Nthenge-Ngumbau DN, Singh R, Kankanala T, Mehta H, et al. Mitochondrial deficits accompany cognitive decline following single bilateral intracerebroventricular streptozotocin. *Curr Alzheimer Res.* 2015; 12:785–795. [PubMed: 26159195]
76. Akinola OB, Biliaminu SA, Adediran RA, Adeniyi KA, Abdulquadir FC. Characterization of prefrontal cortex microstructure and antioxidant status in a rat model of neurodegeneration induced by aluminium chloride and multiple low-dose streptozotocin. *Metab Brain Dis.* 2015; 30:1531–1536. [PubMed: 26307418]
77. Wang JQ, Yin J, Song YF, Zhang L, Ren YX, et al. Brain aging and AD-like pathology in streptozotocin-induced diabetic rats. *J Diabetes Res.* 2014; 2014:796840. [PubMed: 25197672]
78. Salkovic-Petrisic M, Knezovic A, Hoyer S, Riederer P. What have we learned from the streptozotocin-induced animal model of sporadic Alzheimer's disease, about the therapeutic strategies in Alzheimer's research. *J Neural Transm (Vienna).* 2013; 120:233–252. [PubMed: 22886150]
79. de la Monte SM, Tong M2. Brain metabolic dysfunction at the core of Alzheimer's disease. *Biochem Pharmacol.* 2014; 88:548–559. [PubMed: 24380887]
80. de la Monte SM. Therapeutic targets of brain insulin resistance in sporadic Alzheimer's disease. *Front Biosci (Elite Ed).* 2012; 4:1582–1605. [PubMed: 22201977]
81. Peri A, Cellai I, Benvenuti S, Luciani P, Baglioni S, et al. PPARgamma in neuroblastoma. *PPAR Res.* 2008; 2008:917815. [PubMed: 18528516]
82. Rohn TT, Wong SM, Cotman CW, Cribbs DH. 15-deoxy-delta12,14-prostaglandin J2, a specific ligand for peroxisome proliferator-activated receptor-gamma, induces neuronal apoptosis. *Neuroreport.* 2001; 12:839–843. [PubMed: 11277593]
83. Powell WS. 15-Deoxy-delta12,14-PGJ2: endogenous PPARgamma ligand or minor eicosanoid degradation product? *J Clin Invest.* 2003; 112:828–830. [PubMed: 12975467]
84. Amlie IK, Fjell AM. Diffusion tensor imaging of white matter degeneration in Alzheimer's disease and mild cognitive impairment. *Neuroscience.* 2014; 276:206–215. [PubMed: 24583036]
85. Brun A, Englund E. Brain changes in dementia of Alzheimer's type relevant to new imaging diagnostic methods. *Prog Neuropsychopharmacol Biol Psychiatry.* 1986; 10:297–308. [PubMed: 3492011]
86. de la Monte SM. Quantitation of cerebral atrophy in preclinical and end-stage Alzheimer's disease. *Ann Neurol.* 1989; 25:450–459. [PubMed: 2774485]

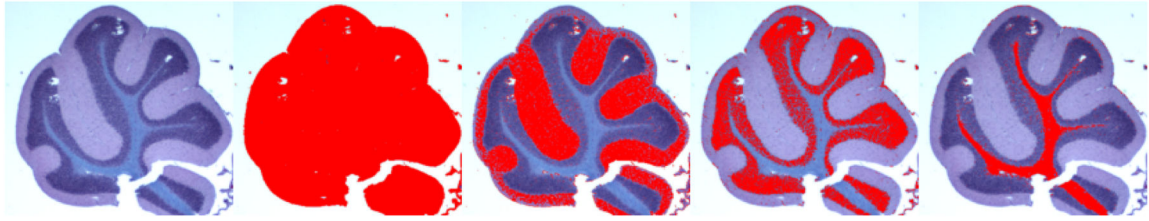


Figure 1.

Image analysis approach. (A) Histological sections of the cerebellar vermis were stained with LHE to highlight the cerebellar cortex and white matter. Image J/Fiji software was used to measure (highlighted in red) (B) Total cross-sectional areas of the vermis, (C) The molecular layer, (D) Granule cell layer, and (E) White matter.

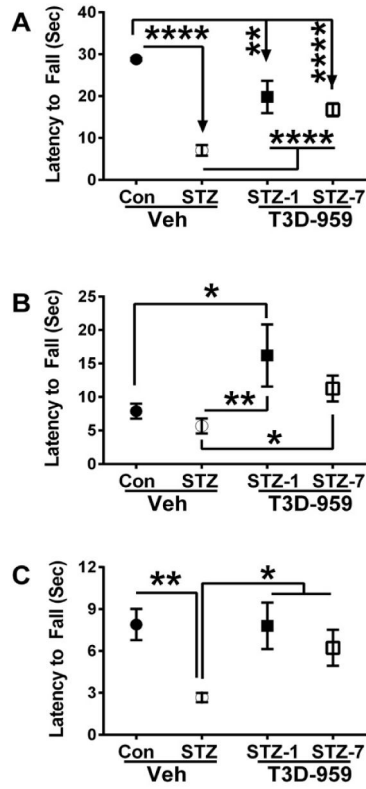


Figure 2.

T3D-959 rescue of i.c. STZ-mediated of motor impairment. Long Evans rats were administered i.c. STZ or normal saline (Control). The control rats and a subset of the i.c. STZ rats were gavaged with saline. Two other sub-groups of i.c. STZ rats were gavaged with a single daily dose of 1.0 mg/kg of T3D-959 beginning 1 day or 7 days after the i.c. STZ injections. Sixteen days later, the rats were subjected to Rotarod testing with 10 incremental speed trials. Latency to fall was measured optically. Data culled from Trials (A) 1–4, (B) 5–6, and (C) 8–10 are depicted in the graphs (mean \pm S.E.M. per group/trial). Inter-group comparisons were made using the Mann-Whitney test. *P<0.05; **P<0.01; ****P<0.0001.

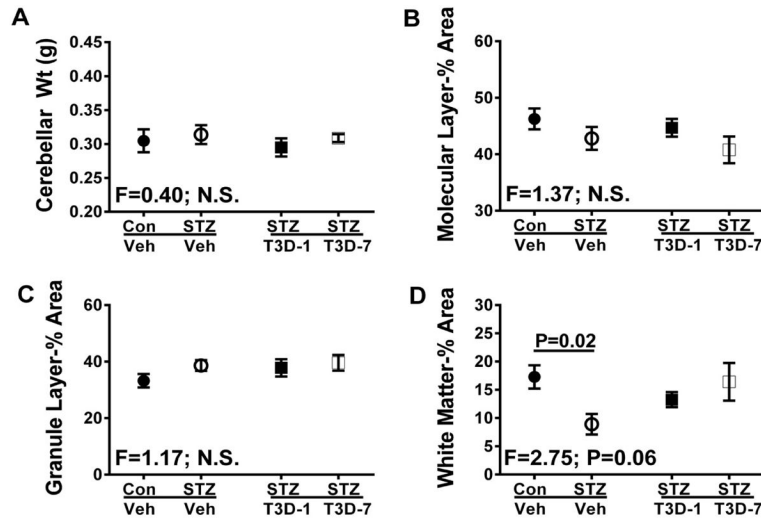


Figure 3. Effects of T3D-959 on i.c. STZ-induced alterations in cerebellar structure. Long Evans male rats (4-weeks old) were used to generate a sporadic model of AD by i.c. STZ. The rats (n=6–8 per group) were treated with saline or 1 mg/kg of T3D-959 by daily oral gavage. Rats were sacrificed on Experimental day 28. (A) Fresh cerebellar weights in rats treated with i.c. saline (Con), ic-STZ (STZ), T3D-959 beginning 1 day after i.c. STZ (STZ T3D-1), or T3D-959 beginning 7 days after i.c.-STZ (STZ T3D-7). After formalin-fixation, cerebella were cut in the mid-sagittal plane and embedded in paraffin. Histological sections (4 μm thick) stained with hematoxylin and eosin (H&E) were used for image analysis (Image-J) to measure relative cross-sectional areas (percentages of overall area) of the (B) molecular layer, (C) granule cell layer, and (D) white matter. All graphs depict the mean ± S.E.M. of results. Inter-group comparisons were made by one-way ANOVA with the Tukey post-hoc significance test. F-ratios are indicated in the panels. Significant inter-group differences are specified.

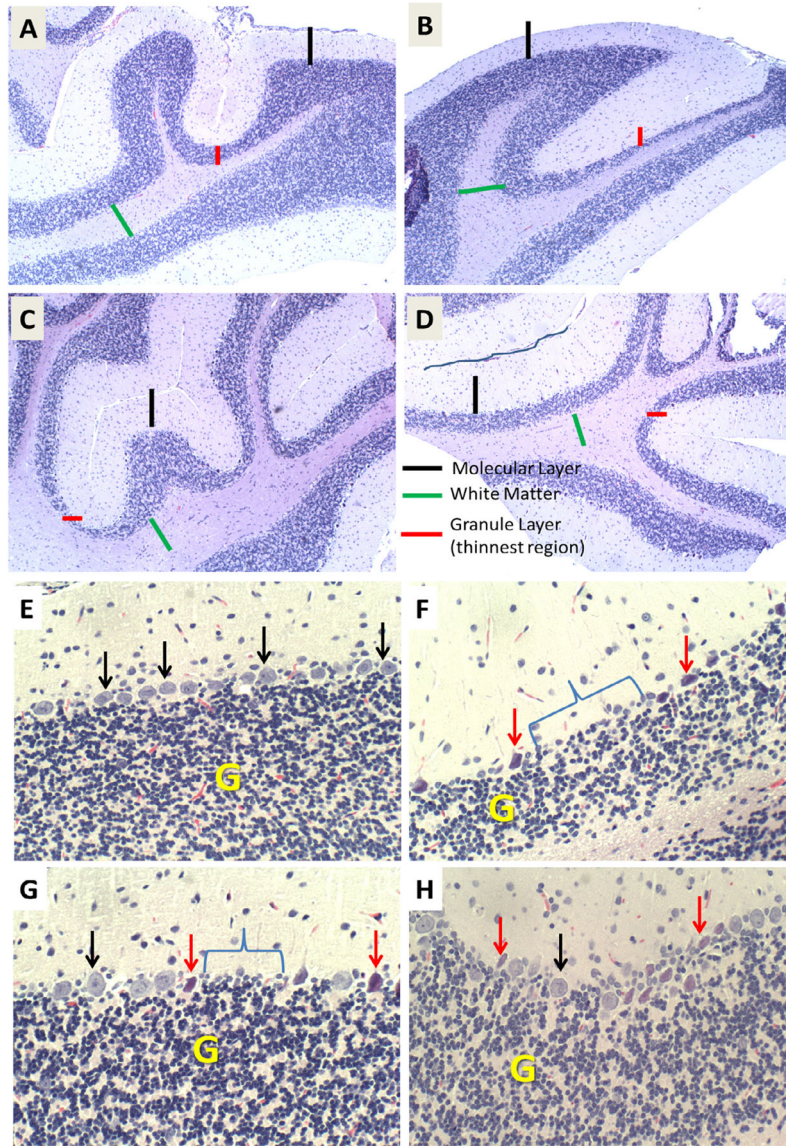


Figure 4. T3D-959 Prevents STZ-induced neurodegeneration. H&E stained sections of the cerebellar vermis from rats treated with (A, E) i.c. saline or (B–D, F–H) i.c. STZ, and then treated with (A, B, E, F) vehicle (saline) or (C, D, G, H) 1 mg/kg/day T3D by gavage. T3D after delays of (C, G) 1 day or (D, H) 7 days. Rats were sacrificed 4 weeks after i.c. STZ or vehicle injections. Cerebella were fixed in formalin, embedded in paraffin and sectioned (4 μm thick). (A, E) Control cerebella had relatively thick and uniform molecular (black bars) and granule cell (red bars, yellow ‘G’), (E) well populated Purkinje cell layers (black arrows), and uniform white matter cores (green bars). Relative to control, i.c. STZ treatment caused cortical atrophy with (B) thinning of the molecular and (B, F) granule cell layers, (F) loss (bracket) and on-going necrosis (red arrows) of Purkinje cells, and modest reductions in white matter thickness. (C, D, G, H) T3D-959 normalized or expanded the molecular layer and increased white matter core thickness, reduced cell loss and necrosis in the Purkinje

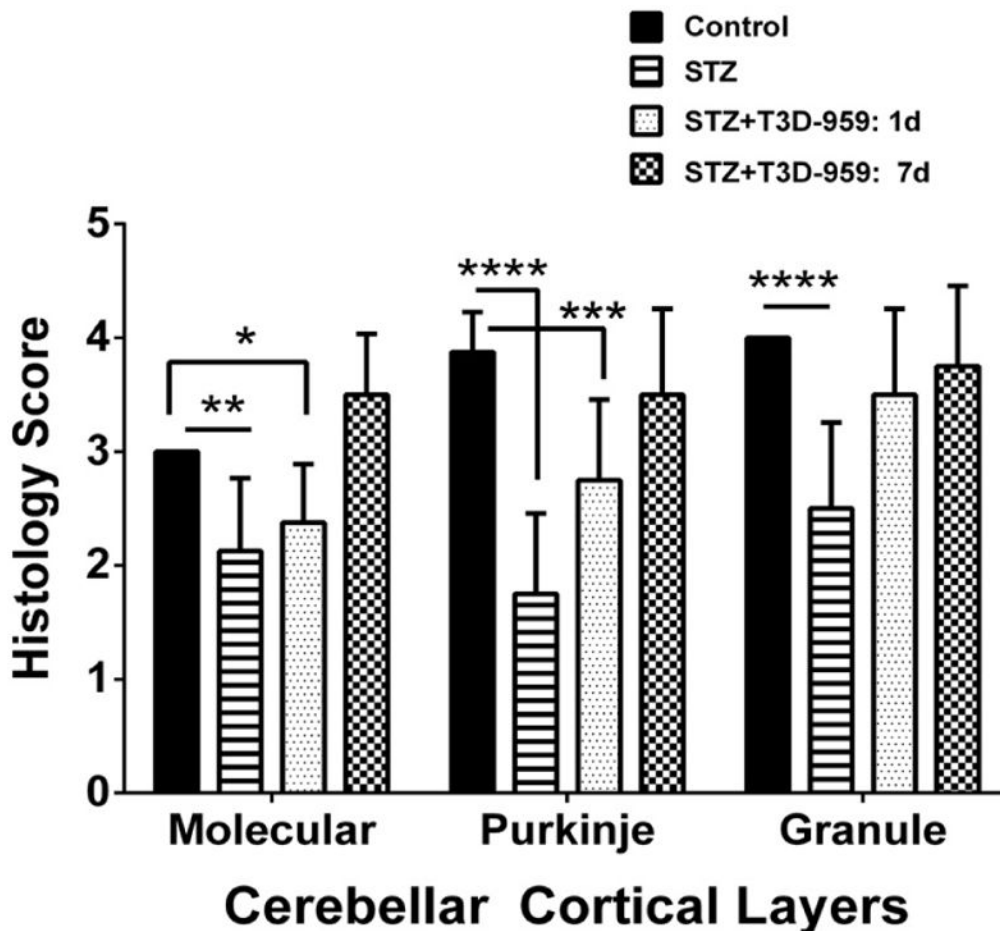
layer, but did not reverse the irregular thinning and neuronal loss in the granule cell layer.
Original magnification: (A–D) 100x; (E–H) 425x.

Author Manuscript

Author Manuscript

Author Manuscript

Author Manuscript



<u>ANOVA table</u>	<u>DF</u>	<u>F (DFn, DFd)</u>	<u>P value</u>
Treatment x Region	9	F (9, 112) = 2.154	P = 0.0305
Treatment	3	F (3, 112) = 44.13	P < 0.0001
Cortical Region	3	F (3, 112) = 10.21	P < 0.0001

Figure 5. Semi-quantitative grading of cerebellar histopathology. H&E stained sections of cerebellar vermis were scored under code using semi-quantitative assessments of the uniformity and thickness of the molecular layer, cellularity within the Purkinje layer, and thickness and cellularity of the granule cell layer (Table 1). The mean ± S.D. scores corresponding were compared across experimental groups by two-way ANOVA (results tabulated below graph) with the Tukey post-hoc multiple comparisons test (*P<0.05; **P<0.01; ***P<0.001; ****P<0.0001).

Table 1

Semi-quantitative grading of cerebellar vermis histopathology.

Cortical Layer	Grade 4	Grade 3	Grade 2	Grade 1
Molecular	Uniformly thick and cellular	Variable thinning, normal cellularity	Variable thinning and reduced cellularity	Uniformly thin
Purkinje	Well populated with histologically intact pyramidal neurons	Isolated neuronal loss or eosinophilic degeneration (necrosis)	Moderate gaps and scattered loss of neurons	Large gaps and conspicuously increased neuronal necrosis
Granule	Uniformly thick and densely cellular	Irregular thinning but densely cellular	Irregular thinning with modest reductions in cell density	Irregular thinning and conspicuous reductions in cell density

H&E stained sections of cerebellar vermis were graded using the semi-quantitative criteria indicated in the table. The mean scores obtained for each layer were compared across the 4 experimental groups by two-way ANOVA (see Figure 5).